AD-A154 521 CALCULATION OF MOLECULAR CONSTANTS POTENTIAL ENERGY CURVES AND FRANCK-CON..(U) AIR FORCE INST OF TECH WRIGHT-PATTERSON AFB OH E A DORKO APR 85 1/1

UNCLASSIFIED AU-AFIT-EN-TR-85-1 F/G 7/4 NL

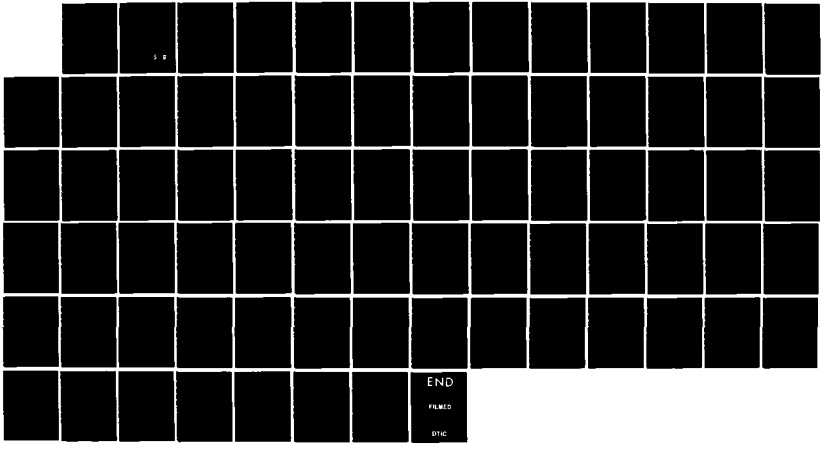

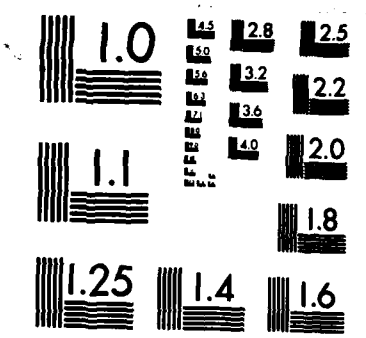

(1)

AU-AFIT-EN-TR-85-1

AIR FORCE INSTITUTE OF TECHNOLOGY

CALCULATION OF MOLECULAR CONSTANTS POTENTIAL ENERGY CURVES AND FRANCK-CONDON FACTORS FOR LEAD OXIDE

ERNEST A. DORKO

SECURITY CLASSIFICATION OF THIS PAGE

REPORT DOCUMENTATION PAGE

1a. REPORT SECURITY CLASSIFICATION Unclassified	1b. RESTRICTIVE MARKINGS
2a. SECURITY CLASSIFICATION AUTHORITY	3. DISTRIBUTION/AVAILABILITY OF REPORT Approved for public release; distribution unlimited/
2b. DECLASSIFICATION/DOWNGRADING SCHEDULE	
4. PERFORMING ORGANIZATION REPORT NUMBER(S) AU-AFIT-EN-TR-85-1	5. MONITORING ORGANIZATION REPORT NUMBER(S)
6a. NAME OF PERFORMING ORGANIZATION School of Engineering 6b. OFFICE SYMBOL (If applicable) AFIT/ENP	7a. NAME OF MONITORING ORGANIZATION
6c. ADDRESS (City, State and ZIP Code) Air Force Institute of Technology Wright-Patterson AFB OH 45433-6583	7b. ADDRESS (City, State and ZIP Code)
8a. NAME OF FUNDING/SPONSORING ORGANIZATION 8b. OFFICE SYMBOL (If applicable)	9. PROCUREMENT INSTRUMENT IDENTIFICATION NUMBER
8c. ADDRESS (City, State and ZIP Code)	10. SOURCE OF FUNDING NOS. PROGRAM ELEMENT NO. / PROJECT NO. / TASK NO. / WORK UNIT NO.
11. TITLE (Include Security Classification) See Box 19	
12. PERSONAL AUTHOR(S) Ernest A. Dorko	
13a. TYPE OF REPORT Summary 13b. TIME COVERED FROM _____ TO _____	14. DATE OF REPORT (Yr., Mo., Day) April 1985 15. PAGE COUNT 76
16. SUPPLEMENTARY NOTATION Keywords:-	Approved for public release IAW AFR 190-17. LYNN E. WOLAVER 15 April 85 Dean for Research and Professional Development Air Force Institute of Technology (AFIT) Wright-Patterson AFB OH 45433
17. COSATI CODES FIELD / GROUP / SUB. GR.	18. SUBJECT TERMS (Continue on reverse if necessary and identify by block number) Chemiluminescence; ~~Lead Oxide~~; Vibronic Spectrum; ~~Franck-Condon Factors~~; Kinetic Mechanism; Flow Tube Reactor; Molecular Constants; Potential Energy Curves.

19. ABSTRACT (Continue on reverse if necessary and identify by block number)

TITLE: Caculation of Molecular Constants, Potential Energy Curves and Franck-Condon Factors for Lead Oxide

ABSTRACT: This paper deals with the preparation of potential energy curves and Franck-Condon factors for diatomic molecules, specifically lead oxide. The starting point for the calculations is the spectroscopic data which can include observations of transitions between rotational, vibrational, and electronic states. Once the data is gathered it can be used to calculate Dunham type coefficients or molecular constants. From these constants the potential energy curve can be calculated by an RKR analysis. From analysis (IPA) the wave functions can be calculated. Finally, Franck-Condon factors can be calculated. Calculations are presented for the diatomic molecule, lead oxide (PbO).

20. DISTRIBUTION/AVAILABILITY OF ABSTRACT UNCLASSIFIED/UNLIMITED ☒ SAME AS RPT. ☐ DTIC USERS ☐	21. ABSTRACT SECURITY CLASSIFICATION Unclassified
22a. NAME OF RESPONSIBLE INDIVIDUAL Ernest A. Dorko	22b. TELEPHONE NUMBER (Include Area Code) (513) 255-2012 22c. OFFICE SYMBOL AFIT/ENP

DD FORM 1473, 83 APR EDITION OF 1 JAN 73 IS OBSOLETE.

UNCLASSIFIED
SECURITY CLASSIFICATION OF THIS PAGE

CALCULATION OF MOLECULAR CONSTANTS POTENTIAL ENERGY CURVES AND FRANCK-CONDON FACTORS FOR LEAD OXIDE

Ernest A. Dorko

Department of Engineering Physics
Air Force Institute of Technology
Wright-Patterson Air Force Base, Ohio, USA

Introduction

This paper deals with the preparation of potential energy curves for diatomic molecules. The starting point for the calculations is the spectroscopic data available which can include observations of transitions between rotational, vibrational, and electronic states. Once this data is gathered, how is it processed so that the entire potential energy curve can be calculated.

Modeling Spectroscopic Data for Diatomic Molecules

Spectroscopic data resulting from the emission of energy by a diatomic molecule during a transition from an excited electronic state to a lower state may be represented as follows:

$$\nu(v',J',v'',J'') = T'(v',J') - T''(v'',J'') \qquad (1)$$

where ν is the observed line frequency in wave numbers, the term values for the upper and lower electronic states, T' and T" respectively, are represented by the Dunham type expression[1]:

$$T(v,J) = {}_i\Sigma_j \, A_{ij}(v + 1/2)^i \, J^j \, (J + 1)^j \qquad (2)$$

Although Eq (2) has the same form as that associated with the Dunham coefficients, Y_{ij}, i.e.,

$$T(v,J) = {}_i\Sigma_j \, Y_{ij}(v + 1/2)^i \, J^j \, (J + 1)^j \qquad (3)$$

researchers M. M. Hessel and C. R. Vidal make the distinction that their A_{ij} values are not necessarily identical to Dunham's Y_{ij}'s.

Dunham[2] arrived at the expression in Eq (2) by using the Wentzel-Kramer-Brillouin method (WKB) to solve the Schroedinger Equation for the rotating diatomic vibrator for the energy levels within one electronic state:

$$\frac{d^2\psi}{d\xi^2} + \frac{8\pi^2\mu r_e^2}{h^2}\left[E - V(\xi) - \frac{h^2 J(J+1)}{8\pi^2 r_e^2 \mu(1+\xi)^2}\right]\psi = 0 \qquad (4)$$

where:

$\xi = (r - r_e)/r_e$

r_e = the equilibrium internuclear separation

μ = the reduced mass

V = the potential of the function, with a minimum at r_e

V_r = the last term which is due to the centrifugal force of rotation.

He expressed the potential energy by expanding V about $\xi = 0$.

$$V = hca_0\xi^2(1 + a_1\ \xi + a_2\ \xi^2 + a_3\ \ \xi^3 + \ldots) \qquad (5)$$

where $a_0 = \omega_e{}^2/4B_e$; ω_e is the classical frequency of small oscillations expressed in cm-1 and $B_e = h/(8\pi^2\mu r_e^2\ c)$. Finally, he obtained expressions for the Y_{ij}'s in terms of the a_k's in Eq (5).

Hessel and Vidal distinguish their constants, A_{ij}, from the Dunham constants, Y_{ij}, by pointing out that the latter are theoretically derived, while the A_{ij}'s are the results of a least-squares fit. Inherent in the least-squares fitting procedure is the fact that the A_{ij} coefficients absorb the effects of inaccuracies in the data, and are somewhat dependent upon the values of their neighboring constants and upon any missing constants[3]. For these reasons, the A_{ij}'s are only estimates of the theoretical Y_{ij} derived by Dunham.

Some further discussion of the A_{ij} and Y_{ij} constants is appropriate. First, a listing of the correspondence of Dunham's

constants and the classical spectroscopic constants is desirable. They are given in Table 1.

TABLE 1

Correspondence Between Dunham Coefficients and Classical Spectroscopic Constants

Y_{00} [a]	$Y_{01} \sim B_e$	$Y_{02} \sim D_e$	$Y_{03} \sim F$	$Y_{04} \sim H$
$Y_{10} \sim \omega_e$	$Y_{11} \sim -\alpha_e$	$Y_{12} \sim \beta_e$		
$Y_{20} \sim -\omega_e x_e$	$Y_{21} \sim T_e$			
$Y_{30} \sim \omega_e y_e$				
$Y_{40} \sim \omega_e z_e$				

(a) Y_{00} is defined as:

$$Y_{00} = 1/4\ Y_{20} + 1/4\ Y_{01}\ ((Y_{11}Y_{10}/(6\ Y^2_{01}) - 1)^2 \qquad (6)$$

This is the expression normally reported in the literature based upon the work of Dunham[2], although the expression for Y_{00} is not explicitly stated in Dunham's work. Sandeman[7] and Jarmain[8] expanded on Dunham's work. Using this material, the expression given in Eq (6) can be verified. In addition to this derivation, the expression for Y_{00} was found in the following works:[9,10,11,12]. The expression for Y_{00} was found to be somewhat different in two publications. First, Herzberg's Y_{00} is

larger than in Eq (6) by +3/4 Y_{20}[13]. Second, in McKeever's work[11] due to a typographical error, "+1/4 Y_{20}" was omitted. The works of Sandeman and Jarmain compliment Dunham's work, making easier the understanding of Dunham's work.

Returning to Eq (1), it should be noted that when a least-squares fit is performed using Eq (2), the bottom of the potential energy curve of the lower state is typically assigned a value of "0". This is done by omitting the A''_{00} term from the fit. When A'_{00} is found from the least-squares fit, it is not equivalent to Dunham's Y'_{00} for the upper state. For this reason, Vidal assigns an asterisk to A'_{00} and calls it A^*_{00}. This term is made up of three components as shown[14]:

$$A^*_{00} = A'_{00} + Te - A''_{00} \tag{7}$$

A'_{00} and A''_{00} are estimated from Eq (6). This A'_{00} and A''_{00} are then the best estimates of Dunham's Y'_{00} and Y''_{00}.Eq (7) can be solved for Te', the electronic term energy of the upper state:

$$Te = A^*_{00} - A'_{00} + A''_{00} \tag{8}$$

In applying Dunham's expression, one should be aware of its limitations. Expressions such as the Morse potential[18]:

$$U(r-r_e) = D_e\ (1 - \exp(-B(r-r_e))^2 \tag{9}$$

are constructed to guarantee that as $r \to r_e$, $U \to 0$ and as $r \to \infty$, U approaches the dissociation energy, D_e. Eq (5) on the other hand does not necessarily satisfy these two criteria. Sandeman showed that if Morse's equation is expanded about $(r-r_e) = 0$, it takes on a form similar to Dunham's Eq (5), but is expressed in terms of two constants and additional numerical coefficients as follows:

$$U = a_0(1 - a + .583a^2\xi - 0.250a^3\xi + 0.086a^4\xi - \ldots) \qquad (10)$$

A comparison of Eqs (5) and (10) shows that Dunham's expression is a more general form of Morse's equation. Sandeman also applied a similar expansion to an equation for potential energy developed by Kratzner[15] and obtained a similar correspondence with Dunham's expression. Because of the increased number of variables and, in turn, the increased flexibility, Dunham's expression has the potential for being more accurate. But, because of this freedom, obtaining constants which satisfy the convergence criterion is more difficult and is not guaranteed for large values of r or v.

Jarmain[8] made a term-by-term comparison of similar expressions developed from Dunham's work and by the RKR method and showed that, upon neglecting Dunham's small corrections, the potentials produced by the two are mathematically identical. Based upon this, the use of Dunham's expression (Eq (3)) to represent spectroscopic data for input to an RKR program for generating potential curves is justified and appropriate.

In applying Dunham's expression, one should remember that his equations are developed for small oscillations about r_e. At energy levels approaching the dissociation limit, Eq (2) may no longer be appropriate. Eqs (1) and (2) are for simple cases. In cases where Λ-type doubling occurs, or where isotopic effects are being considered, more complex models must be substituted for Eqs (1) and (2). Works cited in the bibliography by Vidal and his coworkers present variations of Eq (2).

Spectroscopic Constants by Merging Least-Squares Fit Data

(a) Development of the Method

The large quantity of data obtained in a spectroscopic analysis requires that the data be reduced to a more manageable form. For example, Eqs (1) and (2) in the previous section are used to calculate reportable constants. To make these models usable, the A_{ij} coefficients must be determined. The most widely used method of generating these coefficients is to perform a linear least-squares fit to the experimental data. For spectroscopic data, a model is created, typically involving a power series expansion based upon the rotational and vibrational quantum numbers as expressed in Eqs (1) and (2). If only band head data is being analyzed, the model takes the following form:

$$\nu = {}_i\Sigma_0 A'_{i0} (v' + 1/2)^i - {}_i\Sigma_0 A''_{i0} (v'' + 1/2)^i \qquad (11)$$

If several different transitions are involved, different values of the A" ground state constants may be obtained. In

addition, the accuracy of the A"'s may be different. It is desirable to merge these constants and obtain a best estimate of the ground state constants. This can be done by accomplishing a weighted least-squares fit of the data. Such a merging can produce more accurate estimates of the constants and reduce the error limits associated with them. The merged fit may also improve the upper state constants.

Merging may also be desirable for the case when two groups of data are available with significantly different standard errors. For example, if infrared data for vibration-rotation band transitions and microwave data for transitions between adjacent rotational levels are available, the greater accuracy of the microwave data can improve the accuracy of the other constants if a weighted merged fit is performed.

There are other methods of data fitting available. These methods include least-squares deviation, maximum likelihood, and minimum chi-squared. All have different fit criteria[16]. Also, nonlinear least-squares fits are possible[17,18]. The present report deals only with the least-squares fit techniques.

The least-squares method or "regression" method minimizes the sum of the squared deviations between observed values and values calculated using the constants obtained from the fit. The least-squares method provides the minimum variance linear unbiased (MVLU) estimates of the constants; that is, the least-squares method introduces no bias. The fits produced are linear functions of the data. When the fit is used to reproduce data,

the generated data exhibits the smallest possible variance from the original data that can be achieved with the model and data used[16].

In performing a least-squares fit, the following assumptions are made:

1. The model (equation) chosen to represent the data is a perfect description of the physical event.

2. The model is linear in the constants to be estimated.

3. The mean error of the experimental data is zero. Any systematic error present must be small compared to the variances and random errors of the data.

4. The variance-covariance elements must be finite and their relative values known if different groups of data are to be merged.

In reducing spectroscopic data, three methods are available:

1. The reduction of each band, i.e., each a group of transitions from one electronic state to another, separately.

2. The reduction of a number of bands simultaneously.

3. The reduction of the bands separately and then merging the resulting data.

The first and third techniques are developed in this paper. The method of approach is now described. Least-squares fitting techniques are based upon the following matrix equation:

$$\nu = X\beta + \varepsilon \qquad (12)$$

where ν is a column matrix containing the experimentally observed line frequencies expressed in wavenumbers, X is a matrix made up of the $(v + 1/2)$ and the $J(J + 1)$ terms as dictated by the model in Eqs (1), (2), or (11) as chosen. β is column matrix made up of the A_{ij} constants which are to be calculated. The ε column matrix contains the unknown errors associated with each observed experimental data point.

Eq (12) is then solved for β as:

$$\beta = (X^T X)^{-1} X^T \nu \tag{13}$$

The estimated variance of the fit is expressed as follows:

$$\sigma^2 = (\nu - X\beta)^T(\nu - X\beta)/f_m \tag{14}$$

where f_m is the degree of freedom of the calculation. The degree of freedom, f_m, is equal to the number of experimental values ν used in the fit minus the number of constants to be obtained in the β matrix. The variance-covariance matrix for the constants obtained in Eq (13) is calculated by the following relation:

$$\theta = \sigma^2(X^T X)^{-1} \tag{15}$$

The diagonal elements of the θ matrix are the variances of the constants and the off diagonal elements are their covariances. The correlation between the calculated constants is expressed by the correlation coefficients which are obtained using the variances and covariances in the following manner:

$$C_{ij} = \theta_{ij}/(\theta_{ii}\theta_{jj})^2 \tag{16}$$

X-state with significantly smaller errors than those obtained in separate fits of their data.

The discussion of the b state data was reserved until last, because they were obtained by making reassignments of many transitions that were published in previous works.

The b-state constants listed in Table 2, Column I are based upon the six assignments marked by asterisks in Table 6. The assignments were made by Glessner[25] and Snyder[26] based upon the works of Kurylo, et. al.[30]. The variance of the constants in Table 3 is remarkably small considering that only six data points with five constants were used yielding a degree of freedom of one. A review of Kurylo's tentative assignments[30] and tentative assignments made by Oldenborg, Dickson, and Zare[29] show a much greater difference between the observed and calculated values than would be expected from the constants of Table 2.

Using the b state constants of Table 2, new assignments were made for the experimental data which had been marked as belonging to the b-X transition by Kurylo and Oldenborg. It was possible to make new assignments for 29 of 34 observed values which had been reported as belonging to the b state. Twenty-six of those were used in a least-squares fit to generate new b state constants. DUNCON was used to perform separate least-squares fits to the data of Snyder and Glessner, and to the data of Kurylo and Oldenborg. Then DUNCON was used to merge the results of these fits.

increased error limit reflects a bias in one or both of the data sets.

Column III of Table 3 reflects the most conservative error estimate of the three columns in Table 3. It is also based upon the largest quantity of data.

Presented in Table 5 are the constants obtained by merging the experimental data of Glessner and Snyder. Presented for comparison are results published by other researchers.

The D-state constants were obtained in a separate merged fit from that used to obtain the other constants because of their large error. The values reported by Bloomenthal[28] produced a better fit for his data; hence, his constants are the preferred constants.

The A-state constants reported in Table 5 provide a reasonable agreement with those reported by Linton and Broida[27]. The reported constants are based upon the merging of data reported by Glessner and Snyder.

The small a-state constants reported in Table 5 rival those reported by Linton and Broida in accuracy. Table 3 shows that the merged data of Glessner and Snyder produces constants with error limits of magnitude comparable to that reported by Linton and Broida.

The ground state (X) constants reported in Table 5 agree well with those reported by Linton and Broida. The merging of Glessner's and Snyder's data resulted in constants for the

TABLE 5

Spectroscopic Constants for PbO[3]

Merged onstants	State	Te (cm^{-1})	We (cm^{-1})	WeXe(cm^{-1})
his Study	D	30115.8(46.1)	542.2(54.9)	-1.99(13.1)
Glessner &	B	22282.80(3.67)	489.50(2.63)	0.149(0.363)
nyder, Refs	AO+	19856.22(3.31)	447.88(3.50)	1.013(0.6007)
25) & (26))	b[2]	16335.44(2.89)	428.43(1.21)	-0.99552(0.0983)
	a	16021.51(1.69)	484.239(0.808)	2.949(0.109)
	X		721.905(0.620)	3.5900(0.0683)
inton and	AO+	19862.6(1.5)	444.3(0.8)	0.54(0.12)
roida, Ref	a1	16024.9(1.45)	481.5(0.7)	2.45(0.07)
27)	XO+		720.97(0.36)	3.536(0.025)
loomenthal,	D	30197.0	530.6	1.05
ef (28)	B	22289.8	496.3	2.33
	X		722.3	3.73
ldenborg,	b	16379±430[1]		
ickensen &				
are, Ref (29)				

[1]This value is based upon estimate by Oldenborg, Dickensen and Zare hat the b state is 350±430 cm^{-1} above the a state.

[2]Based upon six data points marked with asterick in Table 7.

[3]Errors reported in parenthesis are one standard deviation.

are the unmerged and merged estimates for the D-X transitions. The D-X data is merged with other data in a separate fit to prevent its large variance from degrading the constants for the other transitions. Finally, the merged results of Glessner and Snyder's data, are compared in Table 5 with the best previous published values available[27,28,29].

Examination of Table 2 reveals values of ω_e for the X-state ranging from 715.7 to 731.5 cm^{-1}. DUNCON permits the merging of the data listed in Table 2 in a weighted-correlated least-squares fashion.

The results of the merging are presented in Table 3. Error limits for ω_e of the X-state are reduced from a maximum standard error of $\pm$11.3 cm^{-1} to $\pm$0.620 cm^{-1} when the data in Columns I and II of Table 2 are merged. The results are presented in Column I, Table 3.

Column II, Table 3 contains the smallest error estimate for the constants of the a-, A-, and X-electronic states. The variances for the merged fits of Columns I and II are similar, 1.0248 and 1.008, respectively. But when the data in Columns I and II are merged to yield Column III, Table 3, the estimated variance of the fit and, in many cases, the standard errors of the individual constants increase. Examination of (Columns I and II) the a- and X-states reveals term electronic energies, T_e with error limits of comparable magnitude which do not overlap. Because of this, when merged, the error limits reflect the equal weighting of the almost significant differences and, hence, the

TABLE 4

Spectroscopic Constants for D-X Transition of PbO (cm^{-1})

Electronic State	Constant	Unmerged	Merged
		[322.3]	[4.19]
D	Te	29897.8(67.4)	30115.8(46.1)
	We'	490.0(30.8)	542.2(54.9)
	We'Xe	-16.53(7.72)	-1.99(13.1)
X	We"	606.1(33.3)	720.989(0.401)
	We"Xe"	-8.32(3.53)	3.5312(0.0296)

Errors Reported in Parenthesis are One Standard Error

TABLE 3

Merged PbO Constants (cm-1)[1]

Electronic State	Constant	Source of Experimental Data: I Merging of Glessner & Snyder Data	II Merging of Linton & Broida Data	III Merging of Glessner, Snyder, Linton, & Broida Data
a	Te	16021.51(1.69)	16024.06(1.16)	16023.16(1.80)
	We'	484.239(0.808)	481.800(0.439)	481.488(0.769)
	We'Xe'	2.949(0.109)	2.4595(0.0434)	2.4339(0.0818)
b	Te	16335.44(2.89)		16331.83(4.77)
	We'	428.43(1.21)		428.34(2.27)
	We'Xe'	-0.99552(0.0983)		-1.014(0.186)
A	Te	19856.22(3.31)	19864.11(2.14)	19860.04(3.13)
	We'	447.88(3.50)	443.39(1.12)	445.32(1.83)
	We'Xe'	1.013(0.6007)	0.446(0.145)	0.655(0.249)
B	Te	22282.80(3.67)		22280.52(7.08)
	We'	489.50(2.63)		489.79(5.25)
	We'Xe"	0.149(0.363)		0.225(0.720)
X	We"	721.905(0.620)	720.736(0.244)	720.890(0.395)
	We"Xe"	3.5900(0.0683)	3.5201(0.0171)	3.5316(0.0292)
Variance of Fit		1.0248	1.008	4.076

[1]Column I is the result of merging with DUNCON the separate fits in Columns I and II of Table 2.

[2]Column II is the result of merging the separate fits in Column III of Table 2.

[3]Column III is the result of merging all separate fits in Table 2 with DUNCON.

Errors reported in parenthesis are one standard error.

TABLE 2 - (Continued)

Electronic Transition	Constant	Source of Experimental Data I Glessner	II Synder	III Linton & Broida
	We'Xe'	2.04(2.74)	0.479(0.8632)	0.443(0.146)
	We"	715.7(11.3)	724.69(2.93)	720.933(0.374)
	We"Xe"	2.80(1.58)	4.012(0.390)	3.5334(0.0239)
		[52.02]	[64.63]	
B-X	Te	22290.9(10.3)	22286.22(9.06)	
	We'	495.70(4.34)	483.00(8.13)	
	We'Xe'	2.22(1.39)	-1.07(1.71)	
	We"	731.52(6.99)	721.11(3.85)	
	We"Xe"	5.06(1.11)	3.532(0.477)	

[1]The quantities in brackets are the variances of the least-squares fits (Eq (14)). Errors reported in parenthesis are one standard deviation. Column I contains least-squares fit to data produced by Glessner (Ref 19). Column II constants are based upon data produced by Snyder (Ref 42). Column II constants are the results of performing least-squares to data published by Linton and Broida (Ref 33).

[2]The constants for b-x were obtained by combining the data observed by Glessner and Snyder.

TABLE 2

Constants from Separate Least-Squares Fits
for Each Electronic Transition (cm^{-1})

Electronic Transition	Constant	Source of Experimental Data I Glessner	II Synder	III Linton & Broida
		[10.03][1]	[9.875]	[6.310]
a-x	Te	16021.54(2.81)	16021.68(2.59)	16023.12(1.38)
	We'	482.93(1.26)	484.51(1.09)	481.831(0.438)
	We'Xe	2.814(0.170)	2.970(0.146)	2.4590(0.0432)
	We"	719.36(2.19)	722.785(0.961)	720.166(0.469)
	We"Xe"	3.067(0.455)	3.712(0.105)	3.4600(0.0462)
		[2.035]		
b-x	Te	16336.43(6.08)[2]		
	We"	428.98(1.46)		
	We'Xe	-0.944(0.114)		
	We"	722.00(1.92)		
	WeXe	3.554(0.193)		
		[41.70]	[33.07]	[4.817]
A-X	Te	19846.0(25.8)	19858.52(6.88)	19864.79(2.38)
	We'	453.5(18.5)	446.30(4.92)	443.31(1.12)

5. The standard error of the constants and the degrees of freedom involved in the calculations. This data will enable the reader to establish his own confidence limits.

6. The estimated variance of the variance, σ_σ, may be helpful. An estimate of this value for large samples of normally distributed data may be obtained by the formula[24].

$$\sigma_\sigma = \sigma/[2f_m]^{1/2} \tag{23}$$

Other data which may be appropriate include the variance-covariance matrix of the final merged constants and the results of the testing to determine the normality of the data sample.

Application to the Spectroscopic Analysis of Lead Oxide (PbO)

The experimental data of the AFIT investigators, Glessner[25], and Snyder[26] was reduced using DUNCON to yield spectroscopic constants for the X, a, b, A, B, and D electronic states of PbO. In addition, the reported data of Linton and Broida[27] was used to obtain constants for the X, a, and A states. The data of Glessner and Snyder was reduced, error estimates were obtained, and the data was merged using DUNCON. Lead-oxide data produced by Linton and Broida was also reduced using DUNCON and the A-X and a-X data were merged. Also, the results of all three investigations were merged using DUNCON. The results of reducing the data of each investigator for each transition separately is presented in Table 2. This data is then merged in several combinations. The constants resulting from these mergings are presented in Table 3. Presented in Table 4

the extension of the potential curve to its dissociation limits[22].

Before merging data from separate least-squares fits, a check should be made for systematic errors. A simple check is to verify that for a given set of confidence limits, say 95%, the error limits for the common constants obtained in two independent fits overlap each other. If they do not, then it is probable that one set contains a systematic error. A second more sophisticated test involves the computation of the confidence limits for the differences for pairs of corresponding constants checking to see if they include zero[16]. Calculation of the confidence limits of differences involves student's t-factor and methods are given by Bennet and Franklin[23]; and Dixon and Massey[20]. A more extensive discussion of the covariance-variance data and how it may be used is presented by Albritton[16,19].

Finally, Albritton provides a recommendation as to what data should be provided in a report on the results of a spectroscopic study. He lists the following as essential data:

1. The observed line numbers (with assignments).
2. If room permits, the variance-covariance matrix used to merge the data.
3. The model used to represent the experimental data.
4. The estimated molecular constants.

With the confidence limits for the estimated constants properly established, one can then determine if the constants are significant[21]. For example, if a constant has a value of 3 and an assigned error limit of ± 5, the range in which the true value of the constant might be found is -2 to +8. This range includes 0; hence, the constant is not significant. If the assigned confidence limits, $\beta_i \pm t\theta_{ii}^{1/2}$ includes zero, then the constant is insignificant and may normally be discarded. Two exceptions to this rule may be encountered.

The first exception concerns the case where a non-zero correlation between two molecular constants exists. If non-zero correlation coefficients are involved, standard errors must be calculated using the most general formulation involving both variances and covariances. If large correlations exist, the rounding of a constant to the number of significant digits dictated by the standard error of the constant, may result in loss of information, i.e., rounding may introduce unnecessary inaccuracies into the calculated data[16].

Albritton suggests that one digit beyond the "one standard error digit" should suffice for most fits. A simple check is to use the rounded constants and see that they reproduce to some desired accuracy the values calculated using the unrounded constants obtained from the fit.

The second exception occurs, where it may prove necessary to retain a constant when not justified by the standard error, in

As in all analyses, the data should be checked to insure that the errors predicted by the least-squares fit follow a normal distribution pattern. Albritton provides a fairly complete discussion of the checks commonly used[16].

Having established that the errors of the data are normally distributed, one should then construct confidence limits for the constants based upon the degrees of freedom and the confidence one wishes to have that the true value is within the assigned limits. The placing of too much reliance upon error limits specified by one standard deviation, $1x\theta_{ii}^{1/2}$, should be avoided. Even if a large sample of data is taken, one can only be about 68% certain that the "true value" lies within a range of $\pm 1x\theta_{ii}^{1/2}$. If a 95% confidence level is desired and the degrees of freedom, f_m, is greater than 30, one must assign limits of $\pm 2x\theta_{ii}^{1/2}$. The multiplier of $\theta_{ii}^{1/2}$ is student's t-factor. It is named after its originator, W. S. Gosset (1876-1937). It is a function of the degrees of freedom of the calculation and the desired confidence level, "1-α". Dixon and Massey (20) give a tabulation of student's t-factor as a function of the degrees of freedom and the degree of confidence. The confidence limits for the constant are then expressed as follows:

$$\beta_i + t(f_m, 1-\alpha)\theta_{ii}^{1/2} \qquad (22)$$

Having established the limits, one can assume that the probability of the true value of falling within the limit $\pm t\theta_{ii}^{1/2}$ is "1-α" where α may vary between 0 and 1.

will hold the desired merged constants. The y matrix will often contain several values for the same constant. Each constant will be represented only one time in the β^M matrix.

To perform a weighted, correlated least-squares fit, a matrix composed of the variance-covariance matrices from a separate least-squares fit is required.

This matrix is given the symbol "θI". It is structured as follows:

$$\theta I = \begin{bmatrix} \theta_1 & 0 & 0 \\ 0 & \theta_2 & 0 \\ 0 & 0 & \theta_3 \end{bmatrix} \tag{18}$$

where θ_1, θ_2, and θ_3 are the variance-covariance matrices of Eq (15). The formula required to obtain the merged constants is as follows:

$$\beta^M = (X^T\theta I^{-1}X)^{-1}\ X^T\theta I^{-1}y \tag{19}$$

The estimated variance of the new merged fit is given by:

$$\sigma^2 = (y - X\beta^M)^T\theta I^{-1}\ (y - X\beta^M)/f_m \tag{20}$$

where f_m is the degree of freedom. The variance-covariance matrix of the merged constants is obtained by the following calculation:

$$\theta^M = \sigma^2(X^T\theta I^{-1}X)^{-1} \tag{21}$$

The subscripts refer to the two constants for which the coefficient expresses the correlation.

As mentioned earlier, the performance of separate fits to each band will yield several values for the constants associated with the lower electronic state. The variances for different bands may also differ significantly. If the variances of the bands are the same, the data can be combined in one large data group and reduced simultaneously. If estimates of the errors are available, a weighted fit based upon the error may and should be performed.

Albritton describes an approach, the correlated least-squares fit, which is more general than the weighted least-squares fit[16,19]. Albritton showed that one need not use all raw data at one time to obtain a merged fit. He showed that a weighted simultaneous multiband fit and a merged band-by-band fit are equivalent. The merged fit is presented in this paper.

The bands or other groups of data are first reduced in a least-squares manner as previously discussed.

Then the data obtained in the initial least-squares fit may be expressed in the following manner:

$$y = X\rho^M + A \tag{17}$$

where y is a column matrix made up of the constants obtained from the separate least-squares fits and ρ^M is a column matrix which

TABLE 6

Assignments of the Vibrational Bands for the b-X Transition of PbO Based on Molecular Constants Obtained by the MVLU Technique

Observed (cm^{-1})	Calculated (cm^{-1})	Obs-Calc (cm)	Assignment	Reference
21643	21659.8	-16.8	14,1	7
21200	21207.6	-7.7	13,1	7
19869.8	19860.2	9.6	10,1*	Present Work
18515	18526.3	-11.3	7,1	2
17488.4	17483.1	5.3	3,0	Present Work
17212	17206.1	5.9	4,1	2
17108	17120.5	-12.5	7,3	2
17033	17047.5	-14.5	2,0	2
16915	16938.0	-23.0	5,2	2
16773	16769.0	4.0	3,1	2
16614	16613.5	-9.5	1,0	2
16488	16499.5	-11.5	4,2	2
16434	16428.7	5.3	7,4	2
16297	16292.4	4.6	17,11	2
16215	16214.1	0.9	14,9	2
16066.8	16062.4	4.4	3,2*	Present Work
15773	15762.0	11.0	13,9	2
15623	15627.0	-4.0	2,2	2
15363	15363.2	-0.2	3,3	2
15281.9	15285.4	-3.5	9,7*	Present Work
14687.8	14671.4	15.6	3,4	Present Work
14180.1	14178.5	1.6	8,8	Present Work
13367.3	13369.4	-2.1	0,4	Present Work
13117.5	13117.4	0.1	1,5*	Present Work
12440.1	12440.4	-0.3	1,6*	Present Work
11968.9	11978.2	-9.3	3,8*	Present Work

The 26 assignments used to obtain the constants are listed in Table 6. The resulting b state and X state constants are presented in Table 7. For the 26 values used in the new fit, a standard error of $\pm$10.5 cm was obtained. For the 15 values which the previous investigators reported "observed-calculated" values, their standard error was $\pm$47.4 cm.

As shown by this example, by use of such a merging technique, a correlation with previous work can sometimes be performed leading to more reliable band assignments.

Rydberg-Klein-Rees Potential Energy Curves

The Rydberg-Klein-Rees (RKR) model for the potential energy curve is developed in this section. Rydberg started with the expression for the total energy, E, for a rotating-vibrating diatomic molecule:

$$E = p^2/2\mu + V(r) \tag{24}$$

The $p^2/2\mu$ term in Eq (24) is the kinetic energy of the system, p in turn, is the linear momentum. The second term, V(r) is defined as follows:

$$V(r) = U(r) + \kappa/r^2 = U(r) + P^2/2\mu r^2 \tag{25}$$

where U(r) is the potential energy of the system, P is the angular momentum of the system, and μ is the reduced mass.

TABLE 7

Spectroscopic Constants for b-X
Transition for Lead Oxide

State	Te	We	WeXe
b	16325.1(11.2)	430.99(2.47)	-0.757(0.165)
X		721.41(4.35)	3.700(0.441)

Based on this energy expression, Rydberg developed a procedure for graphically determining the classical turning points for a diatomic molecule[31]. Klein modified Rydberg's derivation so that the turning points could be calculated numerically[32]. Reese obtained quadratic and cubic analytic solutions approximating Klein's formulas[33].

Klein's mathematical development is given here. Terms used in the development are shown in Fig 1 as an aid in following the presentation. The classical turning points are designed r' and r". Klein defined the turning points in terms of quantities r_1 and r_2. For his analysis, r_1 and r_2 are measured from r_e, r_1 being positive and r_2 negative. Then r' and r" are defined as follows:

$$r' = r_1 + r_e \tag{26}$$

$$r'' = r_e + r_2 \tag{27}$$

Then

$$dr' = dr_1 \tag{28}$$

$$dr'' = dr_2 \tag{29}$$

$$dr = dr_1 \text{ or } dr_2 \tag{30}$$

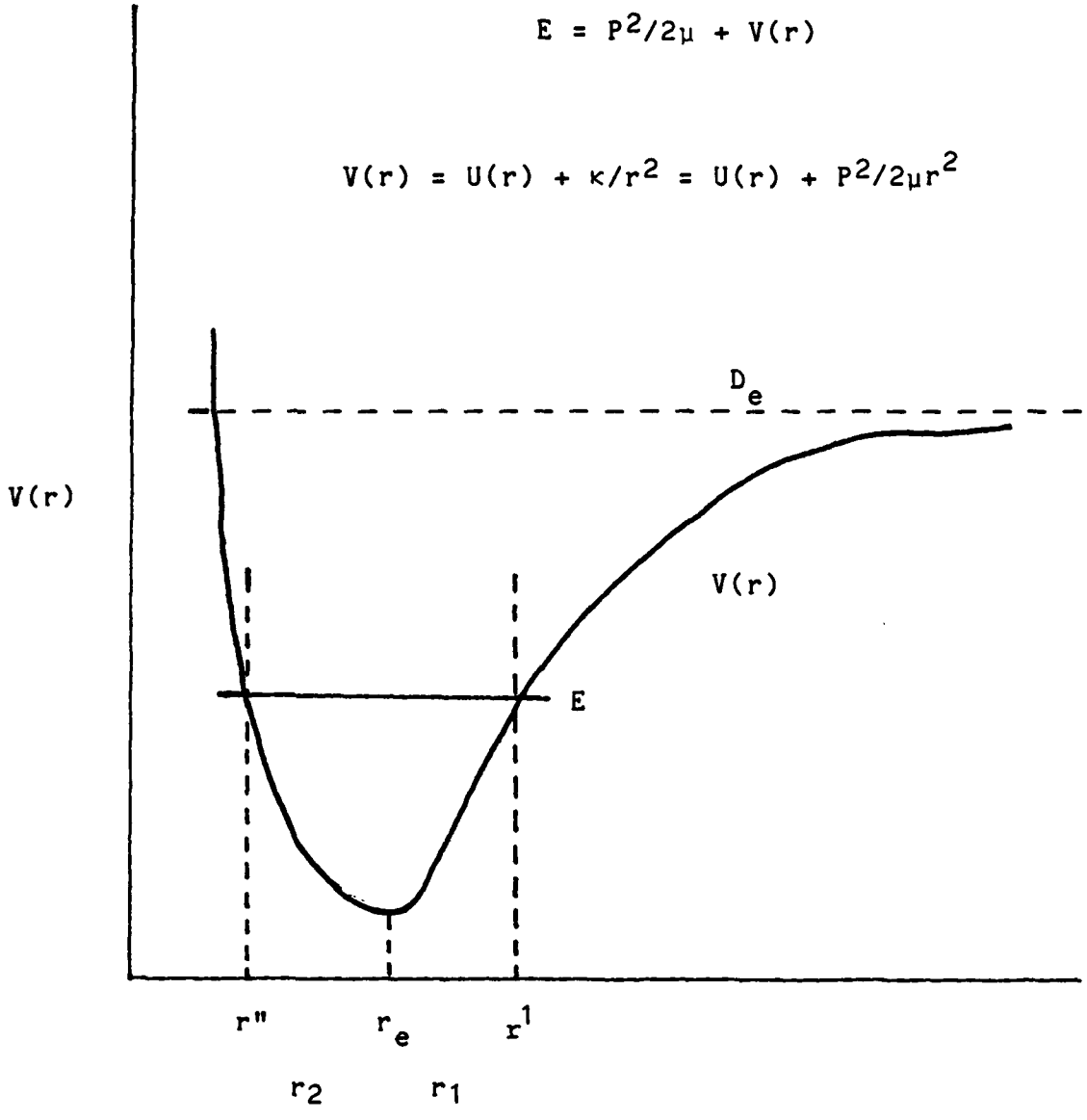

Figure 1. Potential Energy Versus Internulcear Distance for a Diatomic Molecule

Klein designated the width of the potential curve as 2f and from Eqs (26) and (27), it follows that:

$$2f = (r_1 + r_e) - (r_2 + r_e) = r_1 - r_2 \tag{31}$$

The energy in Eq (24) may be expressed as a function of "I", the action integral for a rotating vibrator and "κ". These terms are defined as follows:

$$I = \S P dr \tag{32}$$

$$\kappa = P^2/(2\mu) \tag{33}$$

The following relationships which involve the period, τ, and the average position of a harmonic oscillator, $\overline{1/r}$, are known:

$$1/\tau = \partial E/\partial I \tag{34}$$

$$\overline{1/r^2} = (\partial E/\partial \kappa) \tag{35}$$

$$\rho = \tau(\partial E/\partial \kappa) \tag{35'}$$

Using Eqs (32) and (34) and solving for the differential of E and adding the results, the following is obtained:

$$\delta E = (1/\tau)\delta I + (\rho/\tau)\delta\kappa \tag{36}$$

Inverting Eq (32), the following is obtained:

$$\tau = \partial E/\partial I \tag{37}$$

Setting Eq (36) equal to zero and solving for ρ, the following is obtained:

$$\delta = -\rho I/\partial \kappa \tag{38}$$

From the equation for the momentum, $p = \mu v = \mu(dr/dt)$, one can, by integrating over one cycle, obtain an expression for the period of vibration for a harmonic oscillator:

$$\tau = \S \mu(dr/p) \tag{39}$$

Solving Eq (24), the equation for energy, for p and substituting into Eq (39), the period of oscillation may be expressed as:

$$\tau = (\mu/2) \S (E-V(r))^{1/2} dr \tag{40}$$

The integral in Eq (40) can be broken into two parts, one to be integrated from r_e to r_1, and the other from r_2 to r_e (as depicted in Fig 1). This operation yields:

$$\tau = 2(\mu)^{1/2} \left[\int_{r_e}^{r_1} dr/(E-V(r))^{1/2} - \int_{r_2}^{r_e} dr/(E-V(r))^{1/2}\right] \tag{41}$$

The factor of two is introduced to account for one vibration cycle from r_e through r_1 and r_2 and back to r_e again. Rearranging Eq (41) and recombining the integrals, one obtains:

$$\tau = (2\mu)^{1/2} \int_{r_2}^{r_1} (dr_1 - dr_2)/(E-V(r))^{1/2} \qquad (42)$$

Now to change the variables of integration, Klein defined the following terms:

$$y = V(r) - V(r_e) \qquad (43)$$

and

$$x = E - V(r_e) \qquad (44)$$

where x is constant for a given E. Then r may be expressed as a function of y as follows:

$$r = r_1(y), \; r > r_e \qquad (45)$$

$$r = r_2(y), \; r < r_e \qquad (46)$$

and when at r_e, $r_1(0) = r_2(0) = r_e$. Subtracting Eq (43) from Eq (44):

$$x - y = E - V(r) \qquad (47)$$

and if the "f" of Eq (31) is function of y, then as defined

$$r_1(y) - r_2(y) = 2f(y) \tag{48}$$

then

$$dr_1/dy - dr_2/dy = 2df(y)dy \tag{49}$$

or

$$dr_1 - dr_2 = 2f'(y)dy \tag{50}$$

Using Eqs (45), (46), (47), and (50) to change the variable of integration and integration limits in Eq (42), Klein obtained:

$$\tau = 2\,(2\mu)^{1/2} \int_{y_2}^{y_1} 2\,f'(y)\,dy/(x-y)^{1/2} \tag{51}$$

From Eq (43) when $r = r_e$, then $V(r) = V(r_e)$ and $y = 0$. Thus, the integral in Eq (51) may be evaluated from 0 (defined as the bottom of the potential well) to some value X.

$$\tau = 2\,(2\mu)^{1/2} \int_{0}^{x} f'(y)\,dy/(x-y)^{1/2} \tag{52}$$

This is the first of two integral equations central to Klein's derivation.

Combining Eqs (28), (35), (35'), and (40) yields:

$$\rho = \tau \overline{(1/r^2)} = (\mu/2)^{1/2} \S (1/r^2) [dr/(E-V(r))^{1/2}] \quad (53)$$

By definition:

$$dr/r^2 = -(1/r) \quad (54)$$

Then Eq (53) becomes:

$$\rho = -(\mu/2)^{\frac{1}{2}} \S d(1/r)/(x-y)^{1/2} \quad (55)$$

Again, the integal in Eq (55) may be broken into two parts. Then for $r > r_e$:

$$r'' = r_2 + r_e \quad (56)$$

$$1/r'' = 1/(r_2 + r_e) \quad (57)$$

and if r_e is set equal to 0 then:

$$1/r'' = 1/r_2 \quad (58)$$

Similarily for $r < 0$:

$$1/r' = 1/r_1 \quad (59)$$

Then for small oscillations about r_e, Eq (53) may be written as the difference between the integrals:

$$\rho = 2\,(\mu/2)^{1/2}\left[\int_{1/r_e}^{1/r_1} -d(1/r_1)/(x-y)^{1/2} - \int_{1/r_2}^{1/r_e} -d(1/r)/(x-y)^{1/2}\right] \tag{60}$$

$$\rho = (2\mu)\int_{1/r_2}^{1/r_1} d(1/r_2 - 1/r_1)/(x-y)^{1/2} \tag{61}$$

Klein established the following definition:

$$2g(y) = 1/r_2 - 1/r_1 \tag{62}$$

Differentiating with respect to y yields:

$$2dg(y) = (d/dy)\,(1/r_2) - (d/dy)\,(1/r_1) \tag{63}$$

Changing the notation yields:

$$2g'dy = d(1/r_2) - d(1/r_1) \tag{64}$$

Substituting Eq (64) into Eq (61) yields:

$$\rho = 2\,(2\mu)^{1/2}\int_{\emptyset}^{y}\left[g'(y)dy/(x-y)^{1/2}\right] \tag{65}$$

with the limits of integration assigned in the same manner as for Eq (52). This is the second integral which is central to Klein's derivation.

In the next step of his development, Klein derives expression for r_{max} and r_{min}, the classical turning points for a harmonic oscillator. Klein recognized that the integrals for τ and ρ (Eqs (52) and (65)) were of the Abelian type. He multiplied both sides by $dx/(\alpha-x)^{1/2}$ and integrated both sides from $x = \emptyset$ to $x = \alpha$ where $\alpha = (E - V(r))$ (11), i.e.,

$$\int_{\emptyset}^{\alpha} \tau dx/(\alpha-x)^{1/2} = 2(2\mu)^{1/2} \int_{y=\emptyset}^{y=\alpha} f'dy \int_{x=y}^{x=\alpha} dx/[(\alpha-x)(x-y)]^{1/2} \quad (66)$$

In eq (66)

$$f'(y) = f(\alpha) \quad (67)$$

and

$$\int_{y}^{\alpha} dx/[(\alpha-x)(x-y)] = \int_{y}^{\alpha} dx/(-x^2+y+\alpha-\alpha y)^{1/2} \quad (68)$$

Eq (68) may be integrated as follows (Ref 6:300):

$$dx/(uv)^{1/2} = 2/(bd)^{1/2}\tan^{-1}[(-bduv)^{1/2}/bv], \text{ for } bd > \emptyset \quad (69)$$

e u = a+bx, and v = a'+dx and for the present integral:

a = α a' = -y

b = -1 d = 1

bd = -1

Then the integral can be evaluated to be π.

Finally, the left side of Eq (68) is evaluated as:

$$\int_0^{\alpha} dx/(\alpha-x)^{1/2} = 2(2\mu)^{1/2} f(\alpha) \qquad (71)$$

olving Eq (71) for $f(\alpha)$:

$$f(\alpha) = 1/(2\pi(2\mu)^{1/2}) \int_{\emptyset}^{\alpha} dx/(\alpha-x)^{1/2} \qquad (72)$$

for $\alpha = y$:

$$f(y) = 1/(2\pi(2\mu)^{1/2}) \int_{\emptyset}^{y} dx/(y-x)^{1/2} \qquad (73)$$

Similarily, Eq (65) for g may be transformed into the

owing:

$$g(y) = 1/(2\pi(2\mu)^{1/2}) \int_0^{y} \rho\, dx/(y-x)^{1/2} \qquad (74)$$

From the definitions for x given in Eq (44):

$$dx = dE \tag{74'}$$

stituting Eq (74') into Eq (34) yields:

$$\tau\, dx = dI \tag{75}$$

alling that E is a function of I and κ, and using Eq (47), (73) becomes:

$$f(V) = 1/(2\pi(2\mu)^{1/2}) \int_{\emptyset}^{I} dI/(V-E(I,\kappa))^{1/2} \tag{76}$$

From Eqs (34), (35'), and (74'):

$$dx = \rho\, dE = (\partial E/\partial\kappa)\, dE = \tau(\partial E/\partial\kappa)\,(\partial I/\tau) = (\partial E/\partial\kappa)\partial I \tag{77}$$

Eq (74) becomes:

$$g(V) = 1/(2\pi(2\mu)^{1/2}) \int_{\emptyset}^{I'} \partial[E(I,\kappa)/(\partial\kappa)\, dI]/(V-E(I,\kappa))^{1/2} \tag{78}$$

TABLE 10

RKR and IPA Potential for the a-State of Lead-Oxide

RKR			IPA			
$Gv(cm^{-1})$	R-(Å)	R+(Å)	$Gv(cm^{-1})$	R-(Å)	R+(Å)	$Bv(cm^{-1})X100$
	2.122					
240.13	2.075	2.172	240.23	2.054	2.192	25.163
			716.87	2.011	2.250	24.988
			1188.55	1.982	2.293	24.822
			1655.34	1.960	2.329	24.658
			2117.24	1.942	2.363	24.495
2574.13	1.928	2.394	2574.24	1.925	2.392	24.328
			3026.34	1.911	2.421	24.157
			3473.56	1.899	2.448	23.979
			3915.90	1.887	2.457	23.795
			4353.34	1.877	2.501	23.607
4785.63	1.868	2.528	4785.85	1.868	2.527	23.419
			5213.45	1.859	2.552	23.236
			5636.23	1.850	2.576	23.060
			6054.34	1.842	2.600	22.893
			6467.82	1.834	2.624	22.729
6874.63	1.827	2.647	6876.59	1.827	2.648	22.562
$Y_{00} = 1.5566X10^{-5}$			$Y_{00} = 0.16759$			

TABLE 9

RKR and IPA Potential for Ground State of Lead-Oxide

	RKR			IPA			
	$Gv(cm^{-1})$	R-(Å)	R+(Å)	$Gv(cm^{-1})$	R-(Å)	R+(Å)	$Bv(cm^{-1})X100$
/2		1.921					
	359.62	1.868	1.980	359.918	1.867	1.979	30.687
	1073.52	1.832	2.027	1073.901	1.831	2.027	30.469
	1780.34	1.809	2.062	1780.716	1.808	2.062	30.256
	2480.10	1.790	2.092	2480.445	1.791	2.092	30.048
	3172.78	1.775	2.118	3173.120	1.776	2.119	29.844
	3858.39	1.762	2.143	3858.743	1.763	2.144	29.645
	4536.93	1.751	2.167	4537.299	1.752	2.168	29.452
	5208.40	1.740	2.189	5208.773	1.741	2.190	29.264
	5872.79	1.731	2.211	5873.161	1.732	2.212	29.082
	6530.11	1.722	2.231	6530.471	1.723	2.236	28.905
	7180.36	1.714	2.251	7180.713	1.715	2.253	28.731
	7823.54	1.706	2.271	7823.891	1.707	2.273	28.557
	8259.65	1.699	2.291	8459.997	1.700	2.292	28.378
	9088.68	1.693	2.311	9089.028	1.693	2.311	28.192
	9710.64	1.686	2.330	9711.015	1.686	2.330	27.998
	10325.53	1.680	2.349	10326.059	1.680	2.349	27.796
	Y_{00} = 0.0233501			Y_{00} = 0.37952			

TABLE 8

Input Constants and Data Used to Generate
Potential Energy Curves

nstants	State		
	x	a	A
Te*	0.0	16024.9(1.45)	19862.6(1.5)
Y_{10}*	720.97(0.36)	481.5(0.70)	443.3(0.8)
Y_{20}*	- 3.536(0.025)	- 2.45(0.07)	- 0.54(0.24)
Y_{01}	0.307519**	0.252(0.10)*	0.2588**
Y_{11}	-1.9167×10^{-3}**	-1.6761×10^{-3}#	1.4×10^{-3}**
Y_{02}	2.2×10^{-7}**	2.2×10^{-7}##	3.3×10^{-7}**

Mass : Oxygen - 1.5994 amu; Lead - 207.19 amu.

*Source: Linton and Broida (Ref 33).

**Source: Suchard (Ref 45).

#Source: Calculated from Linton and Broida's Y_{01} using Eq (104).

##Source: Used X-state value for a-state Y_{02}. The a-state Y_{02} should be calculated according to Eq (104'). The error due to this substitution should be small.

Lead-Oxide RKR-IPA Curves

To demonstrate the use of the RKR-IPA program, the x-, a-, and A-states were selected for evaluation. Curves were drawn for the x-, a-, and A-states using the results of the RKR routine alone or using the combined RKR and IPA routine (RKR-IPA curve). The constants used to generate these curves for each state are presented in Table 8. The RKR and IPA results are presented for the X- and a-states in Tables 9 and 10, respectively. The RKR data for the A-state is presented in Table 11. The resulting potential energy curves are presented in Figure 2 for the X-, A-, and the a-states. For the A-state, the curve presented in Figure 2 is an RKR curve, while for the X- and a-states, they are RKR-IPA curves.

The ultimate use of a potential should be to predict what transitions should occur. A sophisticated analysis would involve the calculation of Franck-Condon factors from the wave functions resulting from the solution of the Schroedinger wave equation. But it is possible to arrive at certain conclusions without calculation of the Franck-Condon factors. For example, examination of the a-state and X-state curves show that no overlap exists between the v'=0 energy level for the a-state, and v"=0 for the X-state. This indicates that such a transition is classically forbidden. For example, a transition observed at 15898 cm^{-1} had been assigned to the a-X (0,0) transition. Reevaluation showed that the 15898 band head should be the a-X

part of the present program but are here briefly discussed. One approach Vidal used for quasibound states involved starting the integration of the SWE at small internuclear distances and looking for the maximum of the internal amplitude inside the centrifugal barrier using a Breit-Wigner parametrization[43]. Vidal also used a second approach in the same work[37]. For the quasibound states, he introduced an artificial barrier at large internuclear distances permitting the use of the Numerov-Cooley method. The eigenvalues he found in this manner were slightly higher than the energy eigenvalues derived from the maximum of the internal amplitude. Proper choice of the barrier kept the differences within the standard errors of the measurement. Using this technique, Vidal stated the same numerical method can be used for both quasibound and bound states.

Continuing with the program, as presented in this paper, it is necessary to transform the energy used in the SWE to units which are consistent with the units of length being used, Bohr radii. Thus far, energy has been expressed in terms of inverse centimeters, wavenumbers. To convert wavenumbers to energy units consistent with Bohr radii, it is necessary to divide by this factor[41].

$$\frac{\hbar N_A}{4\pi c a_0 \mu_A} = \frac{60.19972628}{\mu_A} \text{ wavenumbers} \qquad (107)$$

where a = 0.52197706 and N_A = Avogadro's number.

the outer turning points of the rotationless potential. To avoid this, Vidal chose a nonlinear interpolation given by:

$$X = \frac{(r-r_e)(r_{max}-r_{min})}{(r_{max}+r_{min})(r_e+r)-2r_{max}r_{min}-2r_e r} \qquad (105)$$

This relation assumes X=1, for $r=r_e$, and X=0, for $r=r_{max}$ and X=1 for $r=r_{min}$.

The interpolation becomes linear for:

$$r_e = \frac{r_{max}+r_{min}}{2} \qquad (106)$$

This formulation treats the inner and outer turning points with comparable weight and reduces the number of Legendre polynomials in Eq (105).

As noted, the first use of the perturbation technique to adjust approximate potential energy curves is attributed to Hinze and Kosman[36]. The technique used in this program to solve the Schroedinger equation is the Numerov-Cooley method[41,42]. The Numerov-Cooley method of solving the SWE was used by J. K. Cashion to test the validity of approximate eigenvalue equations developed by Perkeris for a rotating Morse oscillator[41].

The routine presented in this paper solves the SWE for bound states. Vidal discusses techniques for handling quasibound states. The techniques for evaluating quasibound states are not

to extend calculations beyond RMII and RMAA, as specified by E_{vJ}, produced large oscillations. He finally settled upon a combination of Legendre polynomials and an exponential function to dampen the oscillations. This combination improved the convergence of the IPA method. The expression Vidal used is as follows[12].

$$V_0(r) = \sum_i c_i P_i(x) \exp(-x^{2n}) \tag{103}$$

where the typical range for n is $1<n<5$. The Gaussian part of Eq (103) provides a smooth cutoff avoiding unphysical oscillations. The Legendre polynomials are calculated using the standard recursion relations[40].

$$(n+1)P_{n+1}(x) = (2n+1)XP_n(x) - nP_{n-1}(x) \tag{104}$$

where $P_1 = 1$ and $P_2 = X$.

Kosman and Hinze[36] used a linear relationship between r and X such that X=1 for $r=4_{max}$ and X=-1 for $r-r_{min}$. Vidal found this relationship to provide poor convergence when dealing with vibrational levels all the way to the dissociation limit and when dealing with anharmonic potentials. He stated that the reason for the poor convergence in the case of a highly anharmonic potential is that a linear interpolation tends to optimize only

$V_{\emptyset}(r)$, being sought may be expressed as a sum of the approximate potential and some delta potential.

$$V_{\emptyset}(r) = V^{\emptyset}_{\emptyset}(r) + \Delta V_{\emptyset}(r) \tag{99}$$

In turn, it follows that the true Hamiltonian differs from the approximate zero order Hamiltonian ($H_o + H_{rot}$) by ΔV (r):

$$H_{\emptyset} + H_{rot} = H_{\emptyset} + H_{rot} + \Delta V_{\emptyset}(r) \tag{100}$$

First order perturbation theory gives the following relationship between the perturbation to the Hamiltonian $\Delta V_{\emptyset}$ (r) and the energy change ΔE_{vJ}:

$$\Delta E_{vJ} = \langle \psi^{\emptyset}_{vJ} \left| \Delta V_{\emptyset}(r) \right| \psi^{\emptyset}_{vJ} \rangle \tag{101}$$

To obtain a correction to V(r), a mathematical expression of the following form is assumed to represent $\Delta V_{\emptyset}$ (r):

$$\Delta V_{\emptyset}(r) = \Sigma c_i f_i(r) \tag{102}$$

The selection of the specific form of the function $f_i(r)$ is critical to the convergence and solution of the SWE.

Kosman and Hinze chose Legendre polynomials $P_i(x)$ to represent the $f_i(r)$ functions[36]. Vidal found that attempting

This formulation has been simplified by neglecting terms describing electronic coupling contributions[39].

The rotational motion of the molecule is described by:

$$H_{rot} = \left[\frac{\hbar}{4\pi\mu c}\right] \frac{J(J+1)}{r^2} \tag{97}$$

In the inverted perturbation approach, one starts with an approximate potential $V_0(r)$, for example an RKR potential. Eq (95) is solved numerically for the zeroth order eigenvalues E_{vJ} and the radial wavefunction $\psi_{vJ}(r)$.

Then an energy correction ΔE_{vJ} is calculated according to the following formula:

$$\Delta E_{vJ} = E_{vJ} - E^0_{vJ} \tag{98}$$

where E_{vJ} is the measured term value as calculated from the spectroscopic constants and quantum numbers v and J. If the difference between the experimentally determined term values and the eigenvalues obtained from the SWE is sufficiently small, the calculation is stopped.

If the difference exceeds a specified limit, then one proceeds. As stated, the goal is to obtain some correction to V(r), i.e., $\Delta V(r)$, such that the calculated and experimental E_{vJ}'s agree. Following this reasoning, then the true potential,

with the SWE. This leads to the use of the inverted perturbation approach. The goal of the inverted perturbation approach (IPA) is to adjust the potential energy curve of rotationless molecules, $V_{\emptyset}(r)$, so that the quantum mechanical eigenvalues, E_{vJ}, obtained from a solution of the Schroedinger wave equation agree in a least-squares sense with the measured term values, $T(v,J)$.

The IPA technique was first demonstrated by Hinze and Kosman[36]. Vidal and Scheingraber[12] expanded the use of the IPA method. Vidal[37,38], in conjunction with several authors, has applied the IPA method to a number of molecules.

The Schroedinger wave equation (SWE) for a vibrating rotator (Eq (4)) is the basis of the IPA method. To develop the IPA method, the SWE can be expressed as follows[12]:

$$(H_o + H_{rot})\psi^{\emptyset}_{vJ}(r) = E^{\emptyset}_{vJ}\psi^{\emptyset}_{vJ}(r) \tag{95}$$

E^{o}_{vJ} is the energy eigenvalue specified by the vibration and rotation quantum numbers. $H_{\emptyset}$ is the Hamiltonian of the nonrotating molecules and is made up of the terms:

$$H_{\emptyset} = -\left[\frac{h}{4\pi\mu c}\right]\frac{d}{dr^2} + V_{\emptyset}(r) \tag{96}$$

where $V_{\emptyset}(r)$ is the potential energy of the rotationless molecule.

Using these definitions, Eq (86) for g becomes:[34]

$$g(v) = \int_{v_0}^{v} B(v')(G(v)-G(v'))^{-1/2}dv' \qquad (93)$$

From the definitions in Eqs (22) and (62) for f and g the following expression for inner and outer turning points may be obtained:

$$r_{\pm} = (f^2 + f/g)^{1/2} \pm f \qquad (94)$$

Solutions of the equations for f and g are discussed in the section on the RKR Program by C. R. Vidal[9]. The Dunham coefficients calculated from spectroscopic constants (i.e., from Program DUNCON) are input to the program, program RIPA. By use of this program the integrations are performed by means of a Gaussian integration routine and an RKR potential energy curve is produced by means of a least squares fit to the inner and outer portions of the curve. These calculations are performed separately for each electronic state of interest.

Inverted Perturbation Analysis

Having constructed a semiclassical RKR curve, the next step is to determine if that curve is consistent with the Schroedinger wave equation; or, even better, to adjust the curve so it agrees

Eq (85) becomes:

$$f = \int_{v_\emptyset}^{v'} (G(v) - G(v'))^{-1/2}\, dv' \tag{88}$$

where Kaiser[35] defined the lower limit of integration by the following:

$$G(v_\emptyset) = -Y_{\emptyset\emptyset} \tag{89}$$

where $Y_{\emptyset\emptyset}$ is the Dunham constant previously defined in Eq (6). The variable $v_\emptyset$ in $G(v_\emptyset)$ may be expressed in terms of Dunham coefficients as:

$$v_\emptyset = -1/2 - \Delta = -1/2\ (Y_{\emptyset\emptyset}/Y_{1\emptyset})(1 + Y_{\emptyset\emptyset}Y_{2\emptyset}/Y_{1\emptyset} + \ldots) \tag{90}$$

For $J = \emptyset$[34]

$$\partial E/\partial J(J+1) = \sum_{n\equiv\emptyset} Y_{ni}(v+1/2)^n = B(v) \tag{91}$$

where B(v) is the spectroscopic term defined as follows:[13]

$$B_v = B_e - \alpha(v+1/2) + \gamma(v+1/2)^2 \ldots \tag{92}$$

Then

$$\partial / \partial\kappa = 2\mu/h^2 (\partial/\partial J(J+1)) \tag{84}$$

Finally, the expressions for f and g become:

$$f(V,J(J+1)) = h/(2\mu)^{1/2} \int_{\emptyset}^{v'+1/2} \frac{d(v+1/2)}{[V-E(v+1/2,J(J+1))]^{1/2}} \tag{85}$$

$$g(V,J(J+1)) = (2\mu)^{1/2}/h \int_{\emptyset}^{v'+1/2} \frac{\partial E/\partial(J(J+1)(v+1/2)^{d(v+1/2)}}{[V-E(v+1/2,J(J+1))]^{1/2}} \tag{86}$$

where the upper limit of integration v' is selected such that $V = E(v'+1/2,J(J+1))$ for the fixed value of J(J+1) used in the integrals [11].

If the RKR calculations are evaluated for J=∅ then Eq (2) reduces to:

$$T = \sum_{i=1} Y_{i\emptyset} (v+1/2)^i = G(v) \tag{87}$$

more commonly referred to as G_v [34].

As $E(I,\kappa)$ approaches V in Eqs (76) and (78), the integrals become infinite. To avoid these singularities, Klein instead evaluated the following expression:

$$S(V,\kappa) = 1/(\pi(2\mu)^{1/2}) \int (V-E(I,\kappa))^{1/2} dI \qquad (79)$$

This expression has the following relation to the f and g of Eqs (76) and (78):

$$f = \partial S/\partial V \; ; \; g = -\partial S/\partial \kappa \qquad (80)$$

As shown in Eq (2), spectroscopic energy levels can be represented as power series of $(v+1/2)$ and $J(J+1)$. It is convenient then to express the integrals for f and g in terms of the quantum numbers v and J.

The expression for the radial action variable in quantum mechanical terms is

$$I = (v+1/2)h \qquad (81)$$

Then

$$d(I) = d(v+1/2)h \qquad (82)$$

The quantum mechanical expression for κ is:

$$\kappa = p^2/2 \approx J(J+1)\ h^2/2 \qquad (83)$$

TABLE 11

RKR Potential for the A-State of Lead-Oxide

V	Gv(cm^{-1})	R-Å	R+Å
0.0	222.30	2.025	2.168
2.5	1328.32	1.937	2.288
5.0	2427.60	1.890	2.367
7.5	3520.12	1.856	2.432
10.0	4605.90	1.829	2.491
12.5	5684.92	1.807	2.546
15.0	6757.20	1.788	2.597

$Y_{00} = 0.28500$

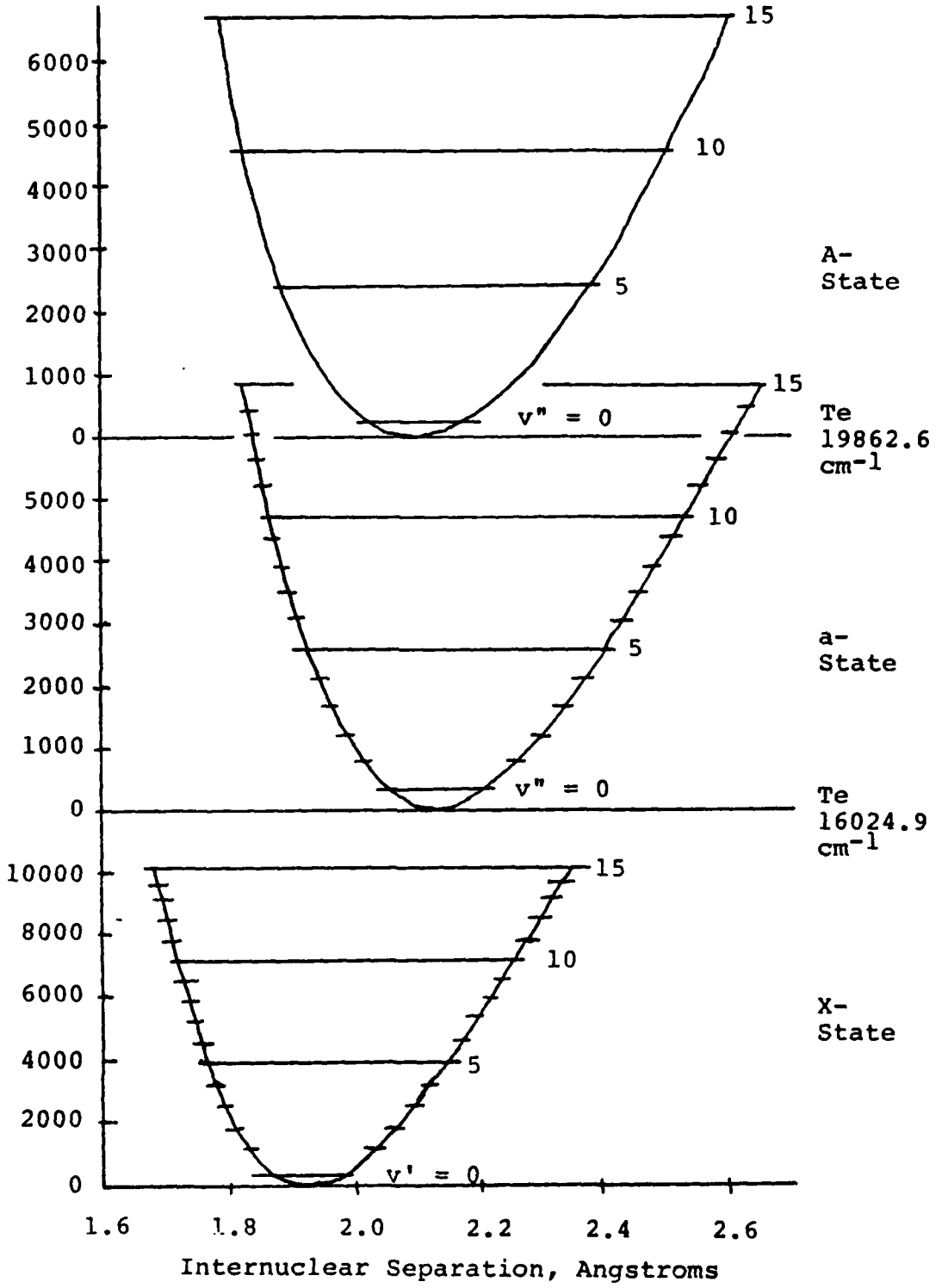

Figure 2. Potential Energy Curves for Lead-Oxide X, a, and A Electronic States

(3,2) transition. Both assignments were acceptable within the error limits of fit. The relative positioning of the potentials indicate that only the (3,2) transition is possible. The calculated value for the a-X (3,2) transition is 15898.4 cm^{-1}.

The next step should be the generation of a new set of constants using the formulas for G_v and B_v and the newly obtained energy eigenvalues G_v and B_v values generated by the IPA routine. This technique was applied to the ground state IPA potential of Table 9. From this, the following constants were generated for the ground state:

$$Y_{10} = 720.991(0.058)\ cm^{-1}$$

$$Y_{20} = 3.5357(0.00479)$$

The calculation of new values for the rotational constants Y_{01}, Y_{11}, etc., from B_v was not performed.

The calculations using only Vidal's RKR-IPA method were halted at this point. Attempts to extend the curves to the dissociation limit in one jump produced a potential which diverged as the curve approached the dissociation limit (see Figure 3). Not having data for vibrational levels above about v=15, the iterative techniques of gradually extending the curve, as discussed by Vidal and Stawalley (Ref 43), were not attempted. They used the IPA method to improve the RKR curve at lower

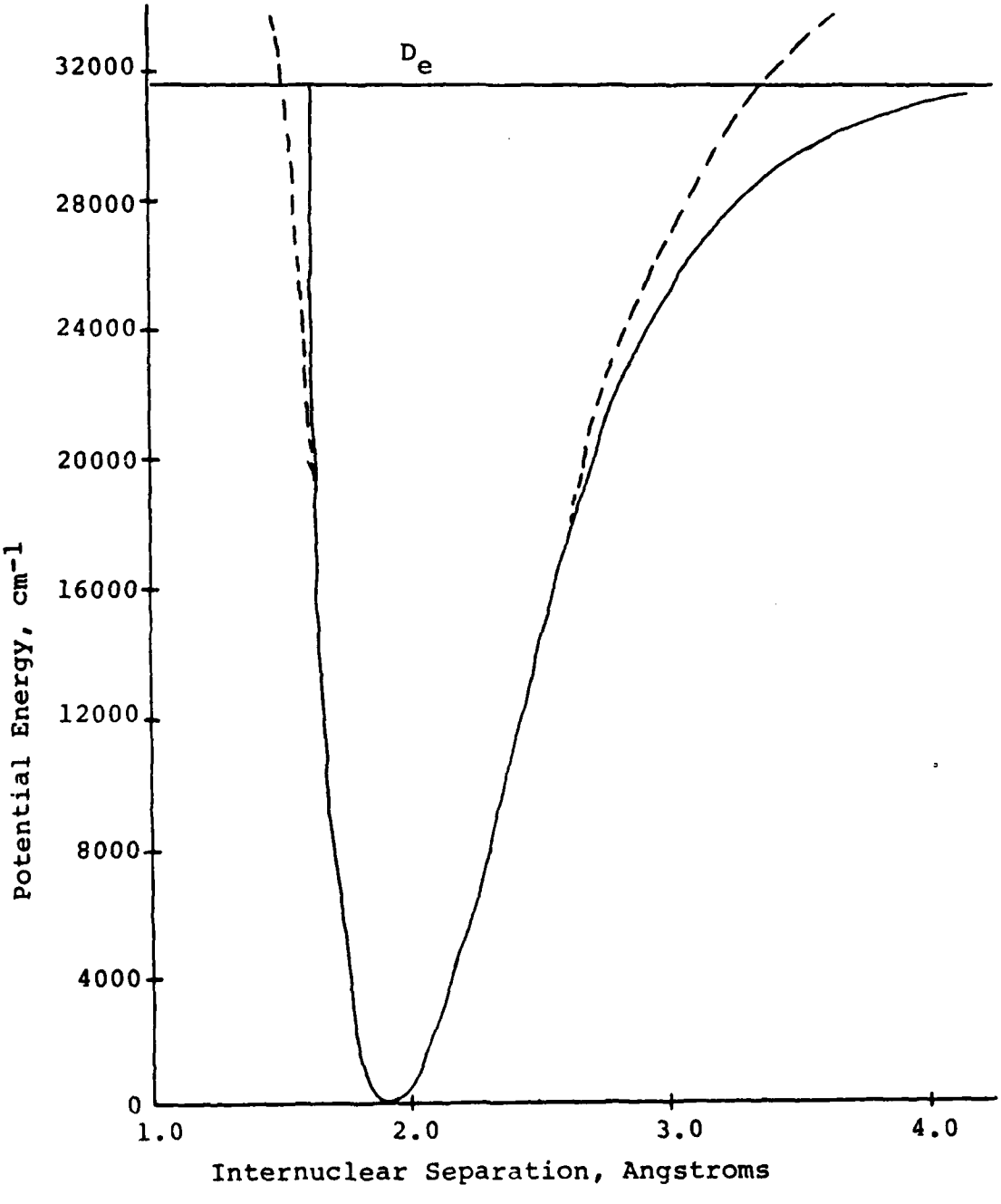

Figure 3. Lead-Oxide X-State Potential Energy Curves

levels, and then on successive trials, extended the curve slowly to the dissociation limit.

The reader is referred to Vidal's works listed in the Bibliography for further information concerning the generation of new constants and the extension of potential curves to the dissociation limit using the IPA routine.

Methods for Extending RKR Curves

In many cases, because of the lack of experimental data, the constants necessary to construct an RKR curve may not be obtainable from straightforward least-square fits or their quality may be insufficient to construct accurate curves. Two techniques for improving existing constants which may, in turn, be used to produced improved RKR curves are presented here[22].

The potential energy curve of a diatomic molecule should have a minimum at some intermediate distance, approach the dissociation limit for large internuclear separations and increase rapidly as the atoms approach each other. Ideally, curves generated using the RKR method should satisfy these criteria.

For many diatomic molecules, only two and, at most, three vibrational constants are available. The available rotational constants are even more limited. Attempts to generate curves based upon these constants using the RKR method can be expected to produce curves which do not meet the dissociation criteria or which do not exhibit an increasing potential for small

internuclear distances. These results occur because the experimental data upon which the constants are based may represent only a fraction of the vibrational levels which exist between the bottom of the potential well and the dissociation limit.

To develop potential energy curves which obey the known constraints, Leroy and Burns have reported on a new technique which shows promising results. While they start with constants obtained from experimentally observed transitions, they then adjust these constants slightly until the new RKR potential energy curve is most consistent with all of the known constraints.

Leroy and Burns used their knowledge of the desired shape to adjust the constants. They worked with the G_v and B_v quantities as expressed in Eqs (87) and (91). Expressed in terms of these two quantities, their criteria for adjusting the molecular constants are:

1. V( ) assymptotically approaches the dissociation energy (De) and the difference between energy levels, $G_{v+1/2}$, becomes Ø for the same value of v. $G_{v+1/2}$ is defined as:

$$G_{v+1/2} = G(v + 1) - G(v) \qquad (108)$$

2. The slope of the inner portion of the RKR curve must be negative. Hence:

$$dV(r)/dr < Ø \qquad (109)$$

3. The slope of the inner portion of the curve must become increasingly steeper; that is, the second derivative with respect to the internuclear separation must be positive:

$$d^2V(r)/dr^2 > 0 \qquad (110)$$

A study of Eq (88) reveals that as $G_{v+1/2}$ becomes smaller, the quantity f becomes larger. In turn, Eq (93) shows that f determines the width of the RKR curve. Examination of Eq (93) further reveals that the value g determines the center of the potential curve for a given energy level. In turn, Eq (92) shows that having determined the constants necessary to generate the G(v)'s, the other factor affecting the value of g is B(v), a quantity whose value is determined by the rotational constants, Y_{ni}. From Eqs (88), (92), and (93), it follows that the width of the curve, as determined by the RKR method, and the value at which $G_{v+1/2} = 0$ depends only upon the vibrational constants which make up Gv. On the other hand, having selected suitable constants for Gv, the behavior of g, the rate at which the outer portion of the curve approaches D_e, and the behavior of the slope of the inner portion of the curve depends solely upon the constants which constitute B_v.

Following this logic, Leroy applied the criteria in 1 above first. If the constants obtained from experimental data do not satisfy this criteria, the value of the last experimental

constant is adjusted or a value is selected for the next constant, $Y_{n\emptyset}$, in the series given by expression (8). The contribution from that constant, $Y_{n\emptyset}(v+1/2)^n$, is then subtracted from the G(v) values calculated from the original experimentally based constants. A least-squares fit is then performed on the adjusted experimental data, Gvj:

$$Gv_j = \sum_{i=1}^{n-1} Y_{i\emptyset} (v_j + 1/2)^i - Y_{n\emptyset} (v_j + 1/2)^n \qquad (111)$$

For a given $Y_{n\emptyset}$ the experimental data fixes the values of the other constants. This new set of constants is tested to determine if Gv approaches a maximum value of D_e. Leroy and Burns say that if this value approaches D_e within <2 cm^{-1} then the criteria in 1 is satisfied. If 1 is not satisfied, then a new trial value for $Y_{n\emptyset}$ is chosen and the process repeated until 1 is satisfied.

At this point, a new RKR curve is generated using the new vibrational constants, $Y_{i\emptyset}$, and the experimental rotational constants, Y_{i1}. The curve is then evaluated according to criteria (2) and (3). If the inner portion of the curve diverges, the process followed for adjusting the constants for Gv is repeated for the constants making up Bv. The value for the last experimental constant is adjusted or a value for the next rotational constant in the Y_{i1} series is selected. Then B_v

values given by the experimental constants are adjusted as follows:

$$Bv_j = \sum_{i=0}^{n-1} Y_{i1}(v_j+1/2)^i - [Y_{n1}(v_j+1/2)^n] \qquad (112)$$

Then a least-squares fit is performed to obtain a new set of rotational constants $Y_{\emptyset 1}$ through Y_{n1}. The new constants are then used to produce a new RKR curve. If the curve does not satisfy the criteria in 2 and 3, then the Y_{n1} constant is adjusted and the process repeated until 2 and 3 are satisfied.

In this manner, Leroy and Burns obtained a set of constants consistent with the experimental data and with criteria 1-3.

Tellinghuisen and Henderson describe a technique for constructing RKR based curves when experimental data does not permit the direct calculation of the rotation constants.[44] Their technique is based upon a combination of the Morse and RKR potentials; hence, Morse-RKR curves.

As explained, vibrational constants provide all the information necessary to calculate f, Eq (88) and, thus, the width of the potential curve, 2f, as defined by Klein for a given vibrational energy level. Having established the width of a potential, the remaining piece of information required to construct a potential curve is the location of either the inner or outer branches of the potential curve, or the center of the potential well, i.e., g as obtained from the RKR calculations.

Tellinghuisen and Henderson point out that inner turning points on a potential curve might be approximated by the Morse potential[13].

$$U(r) = D_e (1 - e^{-\beta(r-r_e)})^2 \qquad (113)$$

where:

D_e = dissociation energy, cm^{-1}

r_e = equilibrium internuclear distance,

$$\beta = 0.12777\ \omega_e (\mu/D_e)^{1/2} \qquad (114)$$

where

ω_e = the vibration frequency, cm^{-1}

μ = reduced mass, amu

Or because of the relation

$$D = \omega_e^2/4(\omega_e x_e) \qquad (115)$$

β may be expressed as follows:

$$\beta = 0.243555\ (\mu\omega_e x_e)^{1/2} \qquad (116)$$

Using these relations, Tellinghuisen investigated 25 different well-known potentials and found errors at the dissociation limit for the inner portion of the curve to be typically less than Ø.Ø2 A and r_e to be in error by seldom more than 1%.

Further, Tellinghuisen states that a potential curve in error by Δr_{min} has identical classical and almost identical quantum eigenvalues for J = Ø. The wavefunctions derived from a shifted curve would be skewed with respect to a proper wavefunction.

If possible, Tellinghuisen recommends the construction of curves by formulas (115) and (116) using the experimental ω_e and $\omega_e x_e$. If only $_e$ and D_e are known, then a value of D_e 4Ø% larger than the experimental D_e should be used.

Tellinghuisen also speculates that α_e might be calculated using an expression derived by Pekeris from the Morse function:(46)

$$\alpha_e = \frac{6\beta_e}{\omega_e}\left[\left(\frac{\omega_e x_e}{\beta_e}\right)^{1/2} - 1\right] \qquad (117)$$

Tellinghuisen found that for 23 of the 25 cases he investigated, the α_e calculated per formula (117) had an average absolute error of 13% and an average signed error of 6%.

If one is seeking the rotational constant D_e (Y_{02}), the following relation might be used:[13]

$$D_e = \frac{4B_e^2}{\omega_e^2} \tag{118}$$

Tellinghuisen cautions against using Bv values made up of only two terms, i.e.,

$$Bv = B_e - \alpha (v+1/2) \tag{119}$$

because the Morse expression for Bv does not terminate with two terms as does Gv. Further, for high values of v, the Morse Bv will differ from the Morse-RKR Bv. The Morse-RKR Bv value must be determined by numerical methods.

b) Extension of the X-State Lead-Oxide Potential Energy Curve to the Dissociation Limit, D_e

The potential energy curve for the ground state of lead-oxide was selected as the likely candidate for extension to the dissociation energy, D_e. This selection was based upon the fact that the constants for the ground state have the smallest standard errors.

The vibrational constants of Linton and Broida were selected as starting values because of their small error limits. The creation of potential energy curves also requires the knowledge

tational constants. The rotational constants were selected
Suchard[45]. Table 12 contains the original constants and
inal set of constants used in extending the curve to the
ciation limit.

The method prescribed by Leroy was used. Linton and Broida's
ants were used to generate a set of G(v)'s according to Eq
for v=Ø to 15. A trial value was selected for $Y_{4Ø}$ and the
constants, $Y_{3Ø}$, $Y_{2Ø}$, and $Y_{1Ø}$ were obtained by performing a
t-squares fit to the value obtained from Eq (111). Program
ON was modified to perform the fit. The process was repeated
l the criterion of $G_{v+1/2} = Ø$ at D_e was satisfied.
Suchard's constants were used to generate a set of B_v's for
to 15 according to Eq (92). A trial Y_{21} was selected and new
and Y_{11} constants were obtained from a least squares fit to
values calculated by Eq (112).

The new vibrational constants and rotational constants were
as the inputs for the RKR-IPA program. The process of
sting the rotational constants was repeated until the
eria expressed in Eqs (1Ø8), (1Ø9), and (11Ø) were satisfied.
The last set of constants calculated are presented in Table
s the extended constants. The Final Set of Turning Points,
utput by the IPA routine was used to create the potential
e (solid line) in Fig 3 which satisfies the dissociation
eria. The dashed line in Fig 3 is the RKR curve, as defined
he original constants of Linton and Broida, and Suchard. It

TABLE 12

Constants Used to Extend the Lead-Oxide X-State Potential Energy Curve to the Dissociation Limit, D_e

Constants	Original Values	Extended Values
Y_{10}	720.97(0.36)	721.062849
Y_{20}	- 3.536	- 3.57101904
Y_{30}		$3.85076374 \times 10^{-3}$
Y_{40}		-1.29×10^{-4}
Y_{01}	0.307519	0.30726775
Y_{11}	-1.9167×10^{-3}	-1.7667×10^{-3}
Y_{21}		-1.5×10^{-5}
Y_{02}	0.22×10^{-6}	0.22×10^{-6}

$D_e = 31570 \pm 410.\ cm^{-1}$

should be noted that the constants, as presented in Table 12, will only produce a curve in Fig 3 when input into an RKR-IPA routine. Examination of the Final Set of Turning Points yields a minimum inner turning radius of about 1.62 angstroms for vibrational quantum numbers from v=33 to v=69. Examination of the turning points for the initial potential generated by RKR, listed at the beginning of the RKR-IPA program output shows RMIN turning points as small as 1.54 angstroms for v=74. For v=69, the last vibrational quantum number investigated by the IPA routine, the RKR program returned an RMIN of 1.59 angstroms. This decreasing value of RMIN indicates that the left branch of the curve would diverge just as shown by the dashed line on the left-hand side in Fig 3. The turning points of the RKR potential were of sufficient quality that the IPA program was able to correct the potential to yield the solid curve of Fig 3. In this work, the procedure described above, was the final one used; however, continued refinements are possible by the use of the RKR-IPA program. The next step should be to take the G(v) [U(R)] and B(v) [BV*100] values as output by the IPA program and perform a least-squares fit to obtain a new set of Y_{n0} and Y_{n1} constants. These, in turn, would be used as input for the constants from the experimental data and to calculate the higher Y_{n+}, ν_+ constants.

The convergence of the IPA routine became very sensitive as the sought for value of the last vibrational constant was

approached. For example, the IPA routine would not converge when values of $Y_{21} = -1.25 \times 10^{-5}$ or $Y_{21} = -1.75 \times 10^{-5}$ were used. The program would converge for values of Y_{21} larger and smaller than these, but the shape of the resulting curve diverged from the desired shape. An indication of the convergence of the IPA routine may be obtained by looking at the next to the last output of the IPA-RKR program, "The Summary of Errors of the Inverted Perturbation Approach."

Due to the fact that the final set of turning points fluctuates about 1.62 angstroms and the potential is in reasing asymptotically along 1.62 angstroms, multiple potential energies are presented for the same RMIN turning point value. Thus, when searches are performed using a turning point radius value [XXX] as in DO-loop 55 of POTTAB, and PLYNN called from this loop, the routine stops at the first value satisfying the requirement [XXX] X(J) (Subroutine PLYNN). The end result is that potential energies corresponding to turning points of magnitude of less than about 1.62 angstroms in the final potential should not be accepted as valid without close inspection. Improved constants and successive iterations of the RKR-IPA routine may remove this discrepancy.

Acknowledgments

I should like to thank the following co-workers for their many excellent contributions to this work:

V. R. Koym, S. R. Snyder, J. W. Glessner, L. L. Rutger, J. Pow, and C. Ritchey.

A portion of this work was supported by a grant from the Air Force Office of Scientific Research under grant number AFOSR/AFIT 83-1.

References

1. C. R. Vidal, Journal of Chemical Physics, 72: 1864-1874, (1980).

2. J. L. Dunham, Physical Review, 41: 721-731, (1932).

3. Merril M. Hessel and C. R. Vidal, Journal of Chemical Physics, 70: 4439, (1979).

4. G. Wentzel, Zeits. f. Physik, 38: 518, (1926).

5. L. Brillouin, Comples Rendus, 183: 24, (1926).

6. H. A. Kramers, Zeits. f. Physik, 39: 828 (1926).

7. W. R. Sandeman, XVII-The Energy Levels of a Rotating Vibrator, "Proceedings of the Royal Society of Edinburgh, Vol. LX: 210-223, (1939-1940).

8. W. R. Jarmain, Canadian Journal of Physics, 38: 217-230, (1960).

9. C. R. Vidal, "RIPA System - Unpublished Computer Program," 1982.

10. Sidney M. Kirshner and James K. G. Watson, Journal of Molecular Spectroscopy, 51, 321-333, (1974).

11. J. W. McKeever and H. C. Schweinler, "Jacobi-Gaus Quandrature Calculations of Rydberg-Klein Potential Energy Curves for Diatomic Molecules and Solutions of the Ensuing Wave

Equations for Some of Their Bound States," Contract No. W-7405-eng-26, ORNL-TM-2167. Oak Ridge, Tennessee: Oak Ridge National Laboratory, (May 1968).

12. H. Scheingraber and C. R. Vidal, Journal of Molecular Spectroscopy, 65: 46-64, (1977).

13. Gerhard Herzberg, Spectra of Diatomic Molecules, New York: McGraw-Hill Book Company, Inc., (1950).

14. W. C. Stwalley and C. R. Vidal, "The $A^1{}^+$-$X^1{}^+$ System of the Isotopic Lithium Hydrides: the Molecular Constants, Potential Energy Curves and Their Adiabatic Corrections," (Paper to be published, 1982).

15. K. Kratzner, Ann. Phys.; Leipzig, Vol. LXVII: 127, (1922).

16. D. L. Albritton, A. L. Schmeltekopf, and R. N. Zare, "An Introduction of the Least-Squares Fitting of Spectrographic Data," Modern Spectroscopy, Modern, Research II, edited by K. Narahari Rao, New York: Academic Press, (1976).

17. Y. Bard, Nonlinear Parameter Estimation, New York: Academic Press, (1974).

18. C. Daniel and F. S. Wood, Fitting Equations to Data, New York: Academic Press, (1974).

19. D. L. Albritton, A. L. Schmeltekopf, and R. N. Zare, Journal of Molecular Spectroscopy, 67: 132-156, (1977).

20. W. J. Dixon and F. J. Massey, Jr., Introduction to Statistics, 3rd ed., New York: McGraw-Hill, (1969).

21. W. H. Kirchoff, Journal of Molecular Spectroscopy, 41: 333-380, (1972).

22. George Burns and Robert J. LeRoy, Journal of Molecular Spectroscopy, 25: 77-85, (1968).

23. C. A. Bennet and N. L. Franklin, Statistical Analysis in Chemistry and the Chemical Industry, New York: Wiley, 1954.

24. W. E. Deming and F. D. Rossini, "The Assignment of Uncertaintities to the Data of Physics and Chemistry with Specific Recommendations for Thermochemistry," Journal of Washington Academy of Sciences, 29: 416-441, (1939).

25. John W. Glessner, Flame Optimization for the Spectroscopic Analysis of the Chemiluminescence from Lead-Oxide, MS Thesis, Wright-Patterson AFB OH: Air Force Institute of Technology, (December 1982).

26. Stephen R. Snyder, Spectroscopic Analysis of PbO Chemiluminescence, MS Thesis, Wright-Patterson AFB OH: Air Force Institute of Technology, (December 1981).

27. C. Linton and H. P. Broida, Journal of Molecular Spectroscopy, 62: 396-415, (1976).

28. S. Bloomenthal, et. al., Journal of Molecular Spectroscopy, 58: 283-300, (1975).

29. R. C. Oldenborg, et. al., Journal of Molecular Spectroscopy, 58: 283-300, (1975).

30. M. J. Kurylo, et. al., Journal of Research of the NBS, 80A, 167-171, (1976).

31. Ragnar Rydberg, Zeit. f. Physik, 73: 376-385, (1932).

32. O. Klein, Zeit. f. Physik, 76: 226, (1932).

33. A. L. G. Rees, Proc. Phys. Soc. (London), 59: 98, (1947).

34. J. N. Huffaker, Journal of Molecular Spectroscopy, 65: 1-19, (1977).

35. E. W. Kaiser, Journal of Chemical Physics, 53: 1986, (1970).

36. Juergen Hinze and Warren K. Kosman, Journal of Molecular Spectroscopy, 56: 93-103, (1975).

37. W. C. Stawalley and C. R. Vidal, "Potential Energy Curves and Adiabatic Corrections of Weakly Bound States," Iowa State Laser Facility and Department of Chemistry and Physics, University of Iowa, Iowa City, Iowa 52242, USA, and Max-Planck-Instit fur Exterrestriche Physik, 8046 Garching, West Germany (Paper to be published 1982).

38. Vidal, C. R., "Precise Determination of Potential Energy Curves from Spectroscopic Data," Max-Planck-Institut fur Physik and Astrophysik Institu fur Extraterrstriche Physik, Garching, West Germany: (to be published).

39. Townes, C. H. and A. L. Schalow, Microwave Spectroscopy, New York: McGraw-Hill, (1955).

40. William H. Beyer, ed. CRC Standard Mathematical Tables (26th Edition), Boca Raton, Florida: CRC Press, Inc., (1981).

41. J. K. Cashion, Testing of Diatomic Potential Energy Functions by Numerical Methods, Journal of Chemical Physics, Vol. 38: 1872-1877, (1963).

42. J. W. Cooley, "An Improved Eigenvalue Corrector Formula for Solving the Schroedinger Equation for Central Fields,"

Mathematics of Computation, Vol. 15, No. 76: 363-374, (October 1961).

43. M. S. Chile, Molecular Collision Theory, Chapter 4, New York: Academic Press, (1974).

44. Stuart D. Henderson and Joel Tellinghuisen, Chemical Physics Letters (to be published 1982).

45. S. N. Suchard, Spectroscopic Data for Heteronuclear Diatomic Molecules, Vol. II, Plenum Publications, (1975).

46. C. L. Perkeris, Physics Review, 45: 98, (1934).

END

FILMED

7-85

DTIC